Macroscopic Experimental and Modeling Evaluation of Selenite and Selenate Adsorption Mechanisms on Gibbsite

Sabine Goldberg*
USDA-ARS
U.S. Salinity Laboratory
450 W. Big Springs Road
Riverside, CA 92507

Selenite Se(IV) and selenate Se(VI) adsorption behavior was investigated on gibbsite as a function of solution pH and solution ionic strength. Adsorption of both Se redox states decreased with increasing solution pH. Electrophoretic mobility measurements showed downward shifts in point of zero charge (PZC) indicative of the formation of inner-sphere Se(IV) and Se(VI) surface complexes. However, the downward shift was less than for strongly adsorbing anions such as phosphate and arsenate, suggesting that outer-sphere surface complexes are also present. The triple layer model, a chemical surface complexation model, was well able to describe Se(IV) and Se(VI) adsorption as a function of solution pH and solution ionic strength by simultaneously optimizing both inner-sphere and outer-sphere surface complexation constants. Direct spectroscopic investigations of selenite surface configuration are needed to corroborate the species suggested by the macroscopic experiments and obtained from the triple layer model optimizations.

Abbreviations: MCL, maximum contaminent level; PZC, point of zero charge.

Selenium is a nutrient element required by animals in trace amounts. It has a very narrow range of sufficiency and becomes toxic at higher concentrations. The maximum contaminant level (MCL) for Se in drinking water has been set at 50 μg L^{-1} by the USEPA (http://water.epa.gov/drink/contaminants/basicinformation/historical/upload/Archived-Consumer-Fact-Sheet-on-Selenium.pdf; aceessed 29 Jan. 2014). In the environment, Se concentrations can become elevated as a result of discharges from refinery and mining operations, disposal of coal and fly ashes, mineral oxidation, dissolution, and drainage of seleniferous soils (Girling, 1984). Bioaccumulation of Se can produce vegetation toxic to grazing animals on seleniferous soils (Lakin, 1961) and vegetation toxic to waterfowl in ponds receiving high Se drainage waters (Ohlendorf et al., 1986).

The predominant Se oxidation states in soil solution, groundwaters, and irrigation waters are selenite, Se(IV) and selenate Se(VI). Selenious acid is a weak diprotic acid with dissociation constants: pK_{a1} = 2.46 and pK_{a2} = 7.31 at 25°C (Weast et al., 1984). Therefore, the dominant selenite species at most natural pH environments are: $HSeO_3^-$ and SeO_3^{2-}. Selenic acid is a strong acid with a second dissociation constant: pK_{a2} = 1.92 at 25°C (Weast et al., 1984). Consequently, the completely dissociated species, SeO_4^{2-} is the only selenate species present at environmental pH values. Selenate is the thermodynamically stable species under oxidizing conditions, while selenite predominates under more reducing conditions (Adriano, 1986). Greater toxicity has been observed for the Se(IV) species

Contribution from the U.S. Salinity Laboratory.
Soil Sci. Soc. Am. J. 78:473–479
doi:10.2136/sssaj2013.06.0249
Received 28 June 2013.
*Corresponding author: (sabine.goldberg@ars.usda.gov).

(Fernandez et al., 1993). The kinetics of Se oxidation–reduction are slow so that both redox states often coexist in environmental solutions (Masscheleyn et al., 1990).

Selenium adsorption reactions have been investigated on a wide range of mineral surfaces including aluminum, iron, manganese, and titanium oxides, clay minerals, and whole soils. Clay minerals and extractable Al and Fe oxides are mineral constituents that were found to be significantly positively correlated with soil Se content (Lévesque, 1974). These minerals can act as sinks that attenuate elevated solution Se concentrations. While the pH dependent adsorption behavior on Fe oxides was similar for both Se redox states with the maximal adsorption occurring at low pH and adsorption decreasing with increasing solution pH; the amount of Se(IV) adsorption was observed to be much greater than that of Se(VI) adsorption (Balistrieri and Chao, 1987; Duc et al., 2003). Similarly, on arid zone soils, Neal and Sposito (1989) observed strong Se(IV) adsorption and virtually no Se(VI) adsorption. However, the opposite was true for Indian soils, where Se(VI) adsorption was consistently greater than Se(IV) adsorption (Singh et al., 1981). On Finnish agricultural soils, some researchers observed Se(VI) adsorption (Vuori et al., 1989, 1994) while another did not (Yläranta, 1983).

Investigations of Se adsorption on Fe oxides have been much more extensive than those on Al oxide minerals. The vast majority of the studies of Se adsorption on Al oxide have been conducted using γ-Al_2O_3 (Ghosh et al., 1994; Wijnja and Schulthess, 2000; Wu et al., 2000, 2001; Boyle-Wight et al., 2002; Elzinga et al., 2009). This synthetic material is manufactured at a high temperature. It is unstable in aqueous solution, dissolving and converting to gibbsite and bayerite, often on the timescale of the adsorption experiment (Goldberg and Glaubig, 1988). Therefore, γ-Al_2O_3 is a poor proxy for gibbsite and amorphous Al oxide, the Al oxide minerals most commonly found in soils. Selenite adsorption has been investigated on gibbsite (Hingston et al., 1972), corundum (Papelis et al., 1995), and amorphous Al oxide (Peak, 2006; Goldberg, 2013), while Se(VI) adsorption has been studied on corundum and amorphous Al oxide (Peak, 2006). As has been observed for Fe oxide minerals, adsorption of both Se redox states on Al oxides was greatest at lower solution pH values and decreased with increasing pH; however, adsorption of Se(VI) decreased much more with increasing solution pH than did Se(IV) adsorption (Ghosh et al., 1994; Wu et al., 2000; Elzinga et al., 2009).

Point of zero charge (PZC) shifts and ionic strength dependence of adsorption behavior are two indirect macroscopic methods for deducing ion adsorption mechanisms on surfaces. Adsorption as a specific inner-sphere surface complex containing no water between the adsorbing ion and the surface functional group produces shifts in PZC. Adsorption as an outer-sphere surface complex containing at least one water molecule between the adsorbing ion and the surface is considered to not produce shifts in PZC (Hunter, 1981). Adsorption of Se(IV) on γ-Al_2O_3 resulted in a pronounced lowering of the PZC, while adsorption of Se(VI) produced no shift (Elzinga et al., 2009). Ions showing decreasing adsorption with increasing ionic strength are considered to be adsorbed as outer-sphere surface complexes, while lack of ionic strength dependence or increasing adsorption with increasing ionic strength indicates ion adsorption as inner-sphere surface complexes (McBride, 1997). Adsorption of Se(IV) on γ-Al_2O_3 showed no ionic strength dependence, while adsorption of Se(VI) decreased with increasing ionic strength (Wu et al., 2000; Boyle-Wight et al., 2002; Elzinga et al., 2009). Thus, both types of experimental observations provide macroscopic evidence of inner-sphere surface complexation for Se(IV) and outer-sphere surface complexation for Se(VI) on Al oxide. These experiments have so far been restricted to Se adsorption by γ-Al_2O_3.

Spectroscopic observations can evaluate adsorption mechanisms directly. Direct spectroscopic evidence for inner-sphere surface complex formation of Se(IV) has been observed on corundum, gibbsite (Papelis et al., 1995), and γ-Al_2O_3 (Elzinga et al., 2009). Selenate was found to adsorb predominantly as outer-sphere surface complexes on γ-Al_2O_3 (Wijnja and Schulthess, 2000; Elzinga et al., 2009) and amorphous Al oxide (Peak, 2006). However, selenate ions on corundum and selenite ions on amorphous Al oxide were found to be mixtures of inner-sphere and outer-sphere surface complexes (Peak, 2006). Therefore, the exact mechanism of surface complexation depends not only on the adsorbing anion species but also on the adsorbent surface.

Selenium adsorption on Al oxide minerals has been described using various chemical surface complexation modeling approaches. Selenium (IV) adsorption on Al oxides has been described using an inner-sphere adsorption mechanism in the constant capacitance model (Goldberg, 1986; Anderson and Benjamin, 1990), the diffuse layer model (Karamalidis and Dzombak, 2010), and the triple layer model (Ghosh et al., 1994; Wu et al., 2000, 2001; Goldberg, 2013). Description of Se(VI) adsorption has been restricted to the triple layer model using outer-sphere surface complexes (Ghosh et al., 1994; Wu et al., 2000, 2001). In their diffuse layer model description, Karamalidis and Dzombak (2010) used the Se(IV) adsorption data of Hingston et al. (1972) but erroneously labeled the result as a Se(VI) surface complexation constant. A clarification of this error is provided in a pdf document entitled Additions and Errata which can be at http://faculty.ce.cmu.edu/karamalidis/files/2012/11/ADDITIONS-and-ERRATA-Gibbsite-Book-2013.pdf (accessed 29 Jan. 2014). Goldberg (2013) included an outer-sphere surface configuration in the description of Se(IV) adsorption on amorphous Al oxide; this surface species only became dominant at solution pH values $\geq$9. Despite spectroscopic evidence that Se(IV) and Se(VI) adsorbs on Al oxides as mixtures of inner-sphere and outer-sphere surface complexes such a combination of surface species has not yet been implemented in a surface complexation model for a crystalline Al oxide mineral.

The objectives of the present study were: (i) to determine Se(IV) and Se(VI) adsorption on gibbsite as a function of solution pH and solution ionic strength; and (ii) to evaluate

for the first time the ability of the triple layer model to describe Se(IV) and Se(VI) adsorption on gibbsite using both inner-sphere and outer-sphere adsorption mechanisms.

MATERIALS AND METHODS

Selenium adsorption was investigated on a hydrated alumina S-11 obtained from the Aluminum Company of America (Alcoa Center, PA). The material was found to consist of gibbsite and showed no detectable impurities with X-ray diffraction powder mounts. Specific surface area was calculated as 18.0 $m^2\ g^{-1}$ using a single-point BET N_2 adsorption isotherm measured with a Quantasorb Jr. surface area analyzer (Quantachrome Corp., Syosset, NY).

Points of zero charge for the gibbsite were determined using a Zeta-Meter 3.0 microelectrophoresis system (Zeta Meter, Long Island City, NY). Electrophoretic mobilities of 0.01% gibbsite suspensions in 0.01 M NaCl solutions were determined at various pH values. Points of zero charge were obtained by linear interpolation of the measurements to zero electrophoretic mobility. Electrophoretic mobilities were also measured in the presence of 19.0 μmol L^{-1} Se(IV) or Se(VI).

Adsorption experiments were performed in batch systems to determine Se adsorption envelopes (amount of Se adsorbed as a function of solution pH per fixed total Se concentration). Samples of 0.2 g gibbsite were added to 250-mL polypropylene centrifuge bottles and equilibrated with 100 mL of a 0.01, 0.1, or 1.0 M NaCl solution by agitating for 20 h on a reciprocating shaker at 23.6 ± 0.1°C. The equilibrating solution contained 19.0 μmol L^{-1} Se(IV) or Se(VI) and had been adjusted to the target pH values using 1.0 M HCl or 1.0 M NaOH that changed the total volume by ≤2%. After reaction, the samples were centrifuged and decanted. The decantate solutions were analyzed for pH, filtered through 0.45-μm membrane filters, and analyzed for Se concentration using inductively coupled plasma optical emission spectrometry. Prior analyses using the direct Se speciation method of Goldberg et al. (2006) had shown no oxidation of Se(IV) to Se(VI) during this reaction period.

For a detailed discussion of the theory and assumptions of the triple layer surface complexation model see Davis and Kent (1990) or Goldberg (1992). The present study employed a combination of inner-sphere and outer-sphere surface complexes to describe Se(IV) and Se(VI) adsorption on gibbsite. Such an approach had previously provided an excellent fit to Se(IV) adsorption by amorphous Al oxide (Goldberg, 2013). In the present application of the triple layer model, the following surface complexation reactions were considered for Se(IV) adsorption:

$$>AlOH + H_2SeO_{3(aq)} \leftrightarrow >AlHSeO_3 + H_2O \quad [1]$$

$$>AlOH + H_2SeO_{3(aq)} \leftrightarrow >AlSeO_3^- + H^+_{(aq)} + H_2O \quad [2]$$

$$>AlOH + H_2SeO_{3(aq)} \leftrightarrow >AlOH_2^+ - HSeO_3^- \quad [3]$$

$$>AlOH + H_2SeO_{3(aq)} \leftrightarrow >AlOH_2^+ - SeO_3^{2-} + H^+_{(aq)} \quad [4]$$

and for Se(VI) adsorption:

$$>AlOH + HSeO_{4(aq)}^- \leftrightarrow >AlSeO_4^- + H_2O \quad [5]$$

$$>AlOH + HSeO_{4(aq)}^- \leftrightarrow >AlOH_2^+ - SeO_4^{2-} \quad [6]$$

where > AlOH represents reactive surface hydroxyl groups on the gibbsite mineral. The Se(VI) component is $HSeO_4^-$ because H_2SeO_4 does not exist in solution. Surface complexation constants for the above reactions are defined for Se(IV) adsorption as:

$$K^{1is}_{Se(IV)}(\text{int}) = \frac{[>AlHSeO_3]}{[>AlOH][H_2SeO_3]} \quad [7]$$

$$K^{2is}_{Se(IV)}(\text{int}) = \frac{[>AlSeO_3^-][H^+]}{[>AlOH][H_2SeO_3]} \exp(-F\psi_o/RT) \quad [8]$$

$$K^{1os}_{Se(IV)}(\text{int}) = \frac{[>AlOH_2^+ - HSeO_3^-]}{[>AlOH][H_2SeO_3]} \exp\left[F(\psi_o - \psi_\beta)/RT\right] \quad [9]$$

$$K^{2os}_{Se(IV)}(\text{int}) = \frac{[>AlOH_2^+ - SeO_3^{2-}][H^+]}{[>AlOH][H_2SeO_3]} \exp\left[F(\psi_o - 2\psi_\beta)/RT\right] \quad [10]$$

and for Se(VI) adsorption as:

$$K^{is}_{Se(VI)}(\text{int}) = \frac{[>AlSeO_4^-]}{[>AlOH][HSeO_4^-]} \exp\left[-F\psi_o/RT\right] \quad [11]$$

$$K^{os}_{Se(VI)}(\text{int}) = \frac{[>AlOH_2^+ - SeO_4^{2-}]}{[>AlOH][HSeO_4^-]} \exp\left[F(\psi_o - 2\psi_\beta)/RT\right] \quad [12]$$

where square brackets indicate the molar concentrations (mol L^{-1}), F is the Faraday constant (C mol_c^{-1}), ψ_o is the surface potential (V) in the o-plane of inner-sphere (*is*) adsorption, ψ_β is the surface potential (V) in the β-plane of outer-sphere (os) adsorption, R is the molar gas constant (J $mol^{-1}\ K^{-1}$), and *T* is the absolute temperature (K). The exponential terms can be considered as solid-phase activity coefficients that correct for the charges on the surface complexes located in each surface plane of adsorption.

The mass balance equation for the surface functional group for Se(IV) adsorption is:

$$\begin{aligned}>AlOH_T = {} & [>AlOH] + [>AlOH_2^+] + [>AlO^-] + [>AlO^- - Na^+] + \\ & [>AlOH_2^+ - Cl^-] + [>AlHSeO_3] + [>AlSeO_3^-] + \\ & [>AlOH_2^+ - HSeO_3^-] + [>AlOH_2^+ - SeO_3^{2-}]\end{aligned} \quad [13]$$

and for Se(VI) adsorption the surface functional group mass balance equation is:

$$\begin{aligned}>AlOH_T = {} & [>AlOH] + [>AlOH_2^+] + [>AlO^-] + [>AlO^- - Na^+] + \\ & [>AlOH_2^+ - Cl^-] + [>AlSeO_4^-] + [>AlOH_2^+ - SeO_4^{2-}]\end{aligned} \quad [14]$$

The total number of reactive surface hydroxyl groups, > $AlOH_T$ (mol L^{-1}), is related to the surface site density, N_s (sites nm^{-2}), by:

$$>\mathrm{AlOH}_T = \frac{SC_s 10^{18}}{N_A} N_s \quad [15]$$

where S is the surface area ($m^2\ g^{-1}$), C_s is the solid concentration ($g\ L^{-1}$), and N_A is Avogadro's number.

The overall charge balance equation is:

$$\sigma_o + \sigma_\beta + \sigma_d = 0 \quad [16]$$

Additional charge balance equations for Se(IV) adsorption are:

$$\sigma_o = [>\mathrm{AlOH}_2^+] + [>\mathrm{AlOH}_2^+ - \mathrm{Cl}^-] - [>\mathrm{AlO}^- - \mathrm{Na}^+] - [>\mathrm{AlSeO}_3] + [>\mathrm{AlOH}_2^+ - \mathrm{HSeO}_3^-] + [>\mathrm{AlOH}_2^+ - \mathrm{SeO}_3^{2-}] \quad [17]$$

$$\sigma_\beta = [>\mathrm{AlO}^- - \mathrm{Na}^+] - [>\mathrm{AlOH}_2^+ - \mathrm{Cl}^-] - [>\mathrm{AlOH}_2^+ - \mathrm{HSeO}_3^-] - 2[>\mathrm{AlOH}_2^+ - \mathrm{SeO}_3^{2-}] \quad [18]$$

and for Se(VI) adsorption are:

$$\sigma_o = [>\mathrm{AlOH}_2^+] + [>\mathrm{AlOH}_2^+ - \mathrm{Cl}^-] - [>\mathrm{AlO}^-] - [>\mathrm{AlO}^- - \mathrm{Na}^+] - [>\mathrm{AlSeO}_4] + [>\mathrm{AlOH}_2^+ - \mathrm{SeO}_4^{2-}] \quad [19]$$

$$\sigma_\beta = [>\mathrm{AlO}^- - \mathrm{Na}^+] - [>\mathrm{AlOH}_2^+ - \mathrm{Cl}^-] - 2[>\mathrm{AlOH}_2^+ - \mathrm{SeO}_4^{2-}] \quad [20]$$

where the surface charges σ_i have units of ($mol_c\ L^{-1}$).

The computer program FITEQL 4.0 (Herbelin and Westall, 1999) was used to fit Se surface complexation constants to the adsorption data. The program uses a nonlinear least squares optimization routine to fit equilibrium constants to experimental data and contains the triple layer surface complexation model of adsorption. In the present application, surface complexation constants for inner-sphere and outer-sphere Se species were optimized simultaneously.

Input parameter values employed in the triple layer model were: surface area, surface site density: N_S = 2.31 sites nm^{-2} (recommended for natural materials by Davis and Kent, 1990), capacitances: C_1 = 1.2 F m^{-2}, C_2 = 0.2 F m^{-2} (considered optimum by Zhang and Sparks, 1990), background electrolyte constants: $\log K_{Na}^{+}(\mathrm{int}) = -8.6$, $\log K_{Cl}^{-}(\mathrm{int}) = 7.5$, protonation constant: $\log K_{+}(\mathrm{int})$ = 5.0, dissociation constant: $\log K_{-}(\mathrm{int})$ = −11.2, (from Sprycha, 1989a, 1989b for Al oxide). This set of parameter values was used previously in the application of the triple layer model to Se(IV) adsorption by amorphous Al oxide (Goldberg, 2013). The criterion used to evaluate goodness-of-fit of model optimizations is the variance parameter, V_Y:

$$V_Y = \frac{\mathrm{SOS}}{\mathrm{DF}} \quad [21]$$

where SOS is the weighted sum of squares of the residuals and DF is the degrees of freedom.

RESULTS AND DISCUSSION

The PZC of gibbsite in the presence of a background electrolyte of 0.01 M NaCl occurred at pH 8.5. Figures 1 and 2 present electrophoretic mobility versus solution pH values obtained for gibbsite on adsorption of Se(IV) and Se(VI), respectively. The PZC values are shifted to lower pH values with anion addition. These observed changes in PZC value are macroscopic evidence of inner-sphere surface complex formation of Se(IV) and Se(VI) on gibbsite (Hunter, 1981). The shift in PZC for Se(IV) adsorption was greater than that for Se(VI) adsorption, indicating stronger adsorption for this anion on gibbsite. These results would indicate that some Se(VI) adsorption occurred via outer-sphere surface complex formation. The shift in PZC for Se(IV) adsorption was less than that observed previously for adsorption of the strongly adsorbing phosphate ion on the same gibbsite (Goldberg, 2010), suggesting that some adsorbed Se(IV) may be present as outer-sphere surface complexes.

Selenium adsorption on gibbsite as a function of solution pH and solution Se concentration is indicated in Fig. 3 for selenite and Fig. 4 for selenate. Values of pH below 2 have been included for theoretical purposes to allow complete definition of the adsorption envelopes and to facilitate surface complexation modeling. Selenite adsorption exhibits maxima near pH 3, decreases with increasing solution pH from pH 4 to 8, and becomes minimal above pH 9. This behavior is in contrast to Se(IV) adsorption on amorphous Al oxide where the adsorption

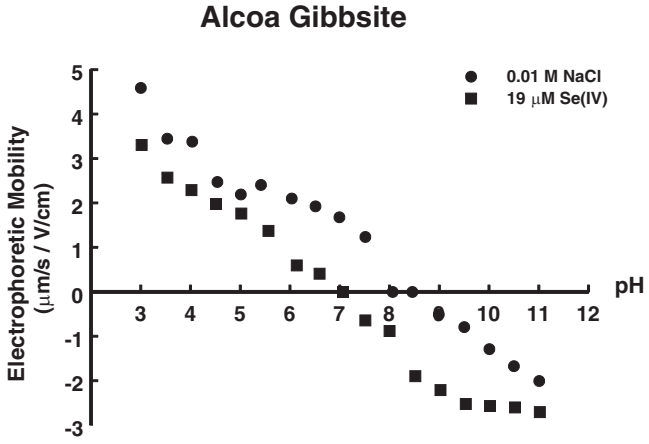

Fig. 1. Electrophoretic mobility of gibbsite as a function of pH and total selenite concentration in 0.01 M NaCl solution. The solid circles represent zero Se(IV) treatment.

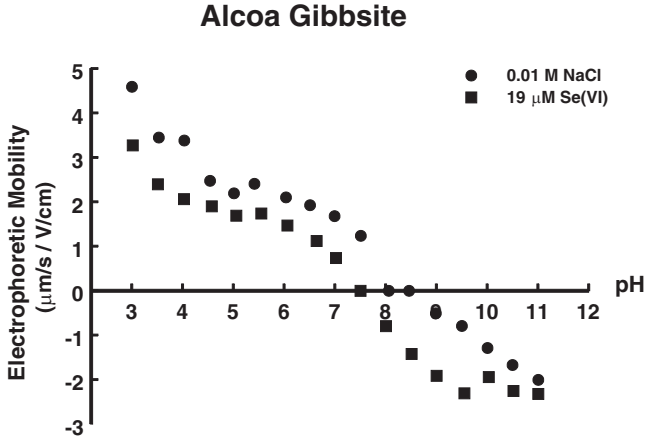

Fig. 2. Electrophoretic mobility of gibbsite as a function of pH and total selenate concentration in 0.01 M NaCl solution. The solid circles represent zero Se(VI) treatment.

maximum was broad and extended up to pH 8 (Goldberg, 2013). These results would suggest that Se(IV) is more strongly adsorbed on amorphous Al oxide than on gibbsite. Ionic strength dependence of Se(IV) adsorption is observed below pH 7 with adsorption decreasing with increasing ionic strength; at solution pH values $\geq$ 7 Se(IV) adsorption is independent of ionic strength (Fig. 3). These results suggest that Se(IV) adsorption occurs via both inner-sphere and outer-sphere surface complex formation on gibbsite.

Selenate adsorption exhibits maxima below pH 3 and decreases with increasing solution pH from pH 3 to 7; minimal adsorption is observed at pH 7 and above. Similar to Se(IV) adsorption, Se(VI) adsorption also exhibits ionic strength dependence at solution pH values below 7 with adsorption decreasing with increasing ionic strength. However, since Se(VI) adsorption is minimal above pH 7. This means that, unlike for Se(IV) adsorption, ionic strength dependent Se(VI) adsorption is observed over the entire pH range where adsorption occurs. These results are macroscopic evidence of outer-sphere surface complexation of Se(VI) on gibbsite. The shape of the Se(VI) adsorption envelope is very similar to that observed for sulfate adsorption on the same gibbsite mineral (Goldberg, 2010).

The ability of the triple layer model to describe Se adsorption on gibbsite is depicted in Fig. 3 for selenite and Fig. 4 for selenate. For Se(IV), the model described the adsorption data quantitatively over the entire pH range (1.5–11) investigated. For Se(VI), the model was able to describe adsorption for the two higher ionic strengths. Deviations of $\leq$1 mmol adsorbed Se(VI) kg^{-1} gibbsite occurred for the lowest ionic strength. The improved model fit for Se(IV) may be due partly to the fact that four surface complexation constants were optimized for Se(IV) adsorption as opposed to only two for Se(VI) adsorption. The triple layer model constitutes an advancement over Langmuir and Freundlich adsorption isotherm approaches which also contain two adjustable parameters, because the empirical isotherm equations cannot describe changes in adsorption occurring with changes in solution pH or solution ionic strength. Table 1 provides values for the optimized Se surface complexation constants.

The Se surface speciations obtained from the triple layer model are presented in Fig. 5 for selenite and Fig. 6 for selenate. For both redox states, outer-sphere surface complexes predominate at pH values > 3. Given that a greater shift in PZC was observed for Se(IV) adsorption than for Se(VI) adsorption, it is surprising that the model optimizations did not indicate greater proportions of inner-sphere surface complexes for Se(IV) over Se(VI). However, since both redox states exhibited pronounced ionic strength dependence of adsorption, it is reasonable that outer-sphere surface complexes predominate in the model description. The Se(IV) adsorption modeling observed for gibbsite was in contrast to amorphous Al oxide where the model results indicated predominance of an inner-sphere surface complex up to pH 9 (Goldberg, 2013). Simultaneous formation of inner-sphere and outer-sphere surface complexes by a very strongly adsorbing anion is not completely unprecedented since it was observed for arsenate adsorption on the crystalline Al oxide, corundum, using X-ray scattering measurements (Catalano et al., 2008). These researchers indicated that previous spectroscopic methods used, such as extended X-ray absorption fine structure and infrared spectroscopy, lack the ability to conclusively identify or rule out the presence of outer-sphere species when inner-sphere species

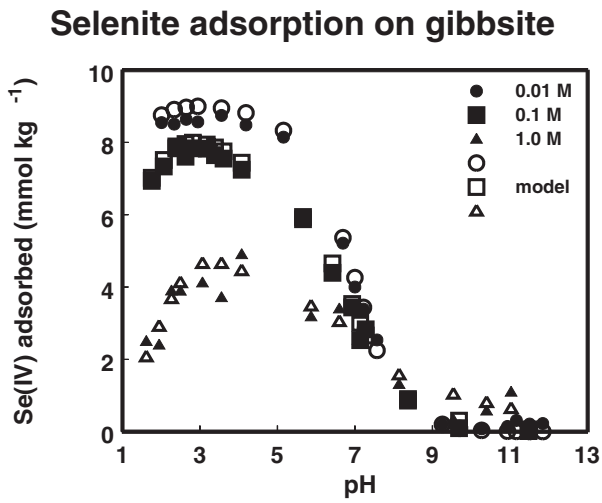

Fig. 3. Fit of the triple layer model to Se(IV) adsorption on gibbsite as a function of solution pH and solution ionic strength from equilibrating solutions of NaCl and Se(IV) = 19 µmol L^{-1}. Experimental data are represented by solid symbols. Model fits are represented by open symbols.

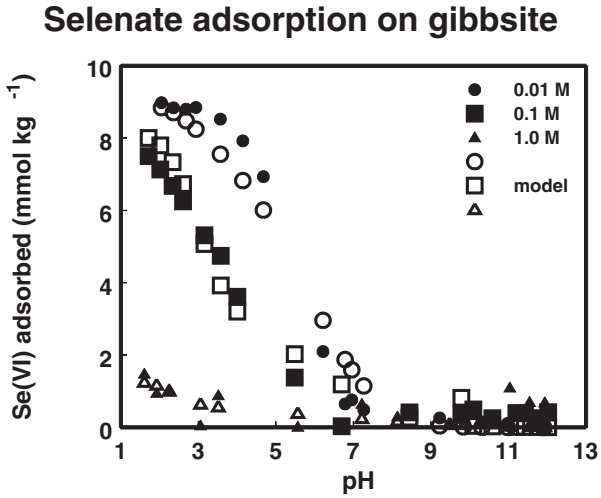

Fig. 4. Fit of the triple layer model to Se(VI) adsorption on gibbsite as a function of solution pH and solution ionic strength from equilibrating solutions of NaCl and Se(VI) = 19 µmol L^{-1}. Experimental data are represented by solid symbols. Model fits are represented by open symbols.

Table 1. Triple layer model selenium surface complexation constants

	Log K^{1is}_{Se}	Log K^{2is}_{Se}	Log K^{1os}_{Se}	Log K^{2os}_{Se}	SOS/DF
Selenite					
0.01 and 0.001 M	4.87	−1.34	8.79	1.80	0.08
1.0 M	4.07		9.06	2.24	1.0
Selenate					
0.01 and 0.001 M		2.91		8.88	1.3
1.0 M		0.039		8.57	1.1

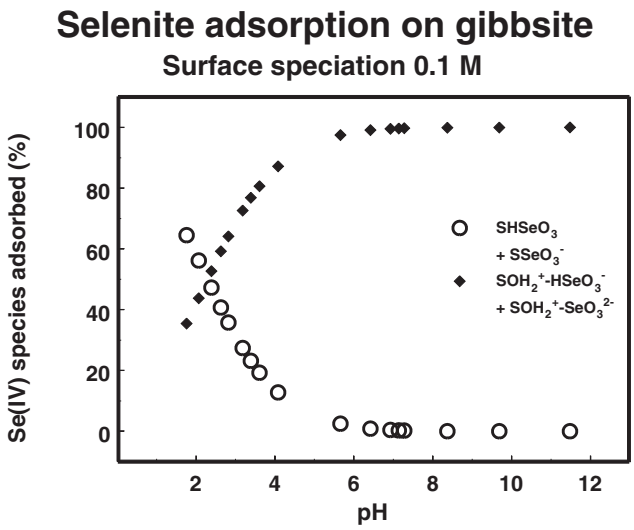

Fig. 5. Surface speciation predicted by the triple layer model for Se(IV) adsorption on gibbsite from equilibrating solutions of 0.1 M NaCl and Se(IV) = 19 μmol L^{-1}. Open symbols represent inner-sphere surface species. Closed symbols represent outer-sphere surface species.

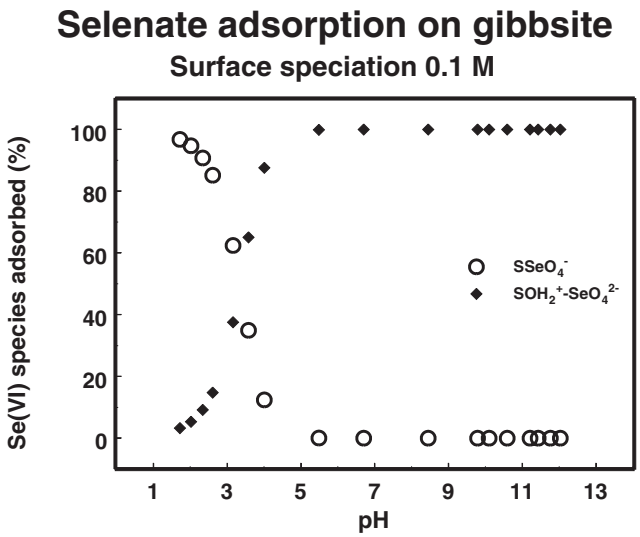

Fig. 6. Surface speciation predicted by the triple layer model for Se(VI) adsorption on gibbsite from equilibrating solutions of 0.1 M NaCl and Se(VI) = 19 μmol L^{-1}. Open symbols represent inner-sphere surface species. Closed symbols represent outer-sphere surface species.

are also present. Therefore, it is possible that anion species previously considered to adsorb exclusively via inner-sphere complex formation were actually adsorbing as a mixture of inner-sphere and outer-sphere surface complexes. This study represents the first surface complexation model application that includes both inner-sphere and outer-sphere surface species to describe Se(IV) and Se(VI) adsorption on a crystalline Al oxide.

Two indirect experimental macroscopic methods were used to deduce Se adsorption mechanisms on gibbsite. Both PZC shifts and ionic strength dependence in adsorption experiments suggested a combination of inner-sphere and outer-sphere surface complexation mechanisms for both Se(IV) and Se(VI) adsorption. Surface complexation modeling results obtained using the triple layer model were in agreement with the macroscopic experiments suggesting predominantly outer-sphere surface complexes for both adsorbed Se(IV) and adsorbed Se(VI) on gibbsite. Direct spectroscopic experimental evidence is necessary to verify the Se surface complexes suggested by our indirect experimental and modeling results. Incorporation of molecular-scale experimental information may improve the chemical significance of the triple layer modeling.

ACKNOWLDEGMENTS

Gratitude is expressed to Ms. P. Xiong and Mr. B. Dao for technical assistance.

REFERENCES

Adriano, D.C. 1986. Trace elements in the terrestrial environment. Springer-Verlag, New York.

Anderson, P.R., and M.M. Benjamin. 1990. Modeling adsorption in aluminum-iron oxide suspensions. Environ. Sci. Technol. 24:1586–1592. doi:10.1021/es00080a020

Balistrieri, L.S., and T.T. Chao. 1987. Selenium adsorption by goethite. Soil Sci. Soc. Am. J. 51:1145–1151. doi:10.2136/sssaj1987.03615995005100050009x

Boyle-Wight, E.J., L.E. Katz, and K.F. Hayes. 2002. Macroscopic studies of the effects of selenate and selenite on cobalt adsorption to γ-Al_2O_3. Environ. Sci. Technol. 36:1212–1218. doi:10.1021/es001775a

Catalano, J.G., C. Park, P. Fenter, and Z. Zhang. 2008. Simultaneous inner-and outer-sphere arsenate adsorption on corundum and hematite. Geochim. Cosmochim. Acta 72: 1986–2004.

Davis, J.A., and D.B. Kent. 1990. Surface complexation modeling in aqueous geochemistry. Rev. Mineral. 23:117–260.

Duc, M., G. Lefevre, M. Fedoroff, J. Jeanjean, J.C. Ruchard, F. Monteil-Rivera, J. Dumenceau, and S. Milonjic. 2003. Sorption of selenium anionic species on apatites and iron oxides from aqueous solutions. J. Environ. Radioact. 70:61–72. doi:10.1016/S0265-931X(03)00125-5

Elzinga, E.J., Y. Tang, J. McDonald, S. DeSisto, and R. Reeder. 2009. Macroscopic and spectroscopic characterization of selenate, selenite, and chromate adsorption at the solid-water interface of γ-Al_2O_3. J. Colloid Interface Sci. 340:153–159. doi:10.1016/j.jcis.2009.08.033

Fernandez, C.M.G., M.A. Palacios, and C. Camara. 1993. Flow-injection and continuous-flow systems for the determination of Se(IV) and Se(VI) by hydride generation atomic absorption spectrometry with on-line prereduction of Se(VI) to Se(IV). Anal. Chim. Acta 283:386–392. doi:10.1016/0003-2670(93)85248-I

Ghosh, M.M., C.D. Cox, and J.R. Yuan-Pan. 1994. Adsorption of selenium on hydrous alumina. Environ. Prog. 13:79–88. doi:10.1002/ep.670130210

Girling, C.A. 1984. Selenium in agriculture and the environment. Agric. Ecosyst. Environ. 11:37–65. doi:10.1016/0167-8809(84)90047-1

Goldberg, S. 1986. Chemical modeling of specific anion adsorption on oxides, clay minerals, and soils. ENVIROSOFT 86. CML Publications, Ashurst, Southampton, UK. p. 671–688.

Goldberg, S. 1992. Use of surface complexation models in soil chemical systems. Adv. Agron. 47:233–329. doi:10.1016/S0065-2113(08)60492-7

Goldberg, S. 2010. Competitive adsorption of molybdenum in the presence of phosphorus or sulfur on gibbsite. Soil Sci. 175:105–110. doi:10.1097/SS.0b013e3181d3462f

Goldberg, S. 2013. Modeling selenite adsorption envelopes on oxides, clay minerals, and soils using the triple layer model. Soil Sci. Soc. Am. J. 77:64–71. doi:10.2136/sssaj2012.0205

Goldberg, S., and R.A. Glaubig. 1988. Boron and silicon adsorption on an aluminum oxide. Soil Sci. Soc. Am. J. 52:87–91. doi:10.2136/sssaj1988.03615995005200010015x

Goldberg, S., D.A. Martens, H.S. Forster, and M.J. Herbel. 2006. Speciation of selenium(IV) and selenium(VI) using coupled ion chromatography—Hydride generation atomic absorption spectrometry. Soil Sci. Soc. Am. J. 70:41–47. doi:10.2136/sssaj2005.0141

Herbelin, A.L., and J.C. Westall. 1999. FITEQL: A computer program for determination of chemical equilibrium constants from experimental data. Rep. 99–01, Version 4.0. Oregon State Univ., Corvallis.

Hingston, F.J., A.M. Posner, and J.P. Quirk. 1972. Anion adsorption by goethite and gibbsite. I. The role of the proton in determining adsorption envelopes. J. Soil Sci. 23:177–192. doi:10.1111/j.1365-2389.1972.tb01652.x

Hunter, R.J. 1981. Zeta potential in colloid science. Principles and applications. Academic Press, London.

Karamalidis, A.K., and D.A. Dzombak. 2010. Surface complexation modeling: Gibbsite. John Wiley & Sons, Hoboken.

Lakin, H.W. 1961. Selenium content of soils In: USDA-ARS Agric. Handb. 200. U.S. Gov. Print. Office, Washington, DC. p. 27–34.

Lévesque, M. 1974. Selenium distribution in Canadian soil profiles. Can. J. Soil Sci. 54:63–68. doi:10.4141/cjss74-008

Masscheleyn, P.H., R.D. Delaune, and W.H. Patrick. 1990. Transformations of selenium as affected by sediment oxidation-reduction potential and pH. Environ. Sci. Technol. 24:91–96. doi:10.1021/es00071a010

McBride, M.B. 1997. A critique of diffuse double layer models applied to colloid and surface chemistry. Clays Clay Miner. 45:598–608. doi:10.1346/CCMN.1997.0450412

Neal, R.H., and G. Sposito. 1989. Selenate adsorption on alluvial soils. Soil Sci. Soc. Am. J. 53:70–74. doi:10.2136/sssaj1989.03615995005300010013x

Ohlendorf, H.M., D.J. Hoffman, M.K. Saiki, and T.W. Aldrich. 1986. Embryonic mortality and abnormalities of aquatic birds: Apparent impacts of selenium from irrigation drainwater. Sci. Total Environ. 52:49–63. doi:10.1016/0048-9697(86)90104-X

Papelis, C., G.E. Brown, G.A. Parks, and J.O. Leckie. 1995. X-ray absorption spectroscopic studies of cadmium and selenite adsorption on aluminum oxides. Langmuir 11:2041–2048. doi:10.1021/la00006a033

Peak, D. 2006. Adsorption mechanisms of selenium oxyanion ions at the aluminum oxide/water interface. J. Colloid Interface Sci. 303:337–345. doi:10.1016/j.jcis.2006.08.014

Singh, M., N. Singh, and P.S. Relan. 1981. Adsorption and desorption of selenite and selenate selenium on different soils. Soil Sci. 132:134–141. doi:10.1097/00010694-198108000-00002

Sprycha, R. 1989a. Electrical double layer at alumina/electrolyte interface. I. Surface charge and zeta potential. J. Colloid Interface Sci. 127:1–11. doi:10.1016/0021-9797(89)90002-7

Sprycha, R. 1989b. Electrical double layer at alumina/electrolyte interface. II. Adsorption of supporting electrolyte ions. J. Colloid Interface Sci. 127:12–25. doi:10.1016/0021-9797(89)90003-9

Vuori, E., J. Vääriskoski, H. Hartikainen, P. Vakkilainen, J. Kumpulainen, and K. Niinivaara. 1989. Sorption of selenate by Finnish agricultural soils. Agric. Ecosyst. Environ. 25:111–118. doi:10.1016/0167-8809(89)90044-3

Vuori, E., J. Vääriskoski, H. Hartikainen, J. Kumpulainen, T. Aarnio, and K. Niinivaara. 1994. A long-term study of selenate adsorption in Finnish cultivated soils. Agric. Ecosyst. Environ. 48:91–98. doi:10.1016/0167-8809(94)90078-7

Weast, R.C., M.J. Astle, and W.H. Beyer. 1984. CRC handbook of chemistry and physics. CRC Press, Inc., Boca Raton, FL.

Wijnja, H., and C.P. Schulthess. 2000. Vibrational spectroscopy study of selenate and sulfate adsorption mechanisms on Fe and Al (hydr)oxide surfaces. J. Colloid Interface Sci. 229:286–297. doi:10.1006/jcis.2000.6960

Wu, C.-H., S.-L. Lo, and C.F. Lin. 2000. Competitive adsorption of molybdate, chromate, sulfate, selenate and selenite on γ-Al_2O_3. Colloids Surf. A Physicochem. Eng. Asp. 166:251–259. doi:10.1016/S0927-7757(99)00404-5

Wu, C.-H., S.-L. Lo, C.F. Lin, and C.-Y. Kuo. 2001. Modeling competitive adsorption of molybdate, sulfate, and selenate on γ-Al_2O_3 by the triple-layer model. J. Colloid Interface Sci. 233:259–264. doi:10.1006/jcis.2000.7223

Yläranta, T. 1983. Sorption of selenite and selenate in the soil. Ann. Agric. Fenn. 22:29–39.

Zhang, P., and D.L. Sparks. 1990. Kinetics of selenate and selenite adsorption/desorption at the goethite/water interface. Environ. Sci. Technol. 24:1848–1856. doi:10.1021/es00082a010